Preliminary interpretative analysis of the QUENCH-18 bundle test using SCDAPSim/mod3.5

Jonathan C. Birchley *, J. Stuckert, M. Steinbrueck, M. Grosse

Karlsruhe Institute of Technology, Institute for Applied Materials Hermann-von-Helmholtz-Platz 1, 76344 Eggenstein-Leopoldshafen, Germany

ARTICLE INFO

Keywords:
Severe accident
SCDAPsim
Air/steam mixture
Nitrogen
Oxidation kinetics
Reflood

ABSTRACT

A preliminary analysis of the bundle reflood experiment QUENCH 18 is performed with the SCDAPSim/Mod3.5/da code containing the PSI developed model for oxidation in the presence of air. The simulation follows on from pre test planning and prediction calculations using the same code and input model. The starting point for the post test calculations differs from the pre test only in respect of using the actual boundary conditions.

Comparison with measured data enables several aspects of the experiment to be studied. Various treatments of steam and air oxidation kinetics investigate the effect of nitrogen on the oxidation and its continuing influence when air is no longer present. Concerning degradation, different assumptions on failure of the oxide crust indicate how the exposure of relocated metallic melt can enhance the oxidation excursion during reflood. Some modelling and knowledge limitations are identified, particularly regarding oxidation in steam air mixtures, the roles of nitrogen and zirconium nitride as chemically active species.

Several observed features of the facility operation remain unresolved. Simulations suggest that damage to the shroud affected the reflood progression. The bundle may also have been in a highly damaged state, with further impacts on reflooding. Interpretation is therefore provisional, pending more information on the bundle final state. However, the simulation results have significant implications for reactor calculations.

1. Introduction

The QUENCH programme (Steinbrück et al., 2010) is being performed at the Karlsruhe Institute of Technology (KIT) to investigate the effectiveness of water injection as a means of reflooding and quenching a core, following a beyond design basis accident with temperatures above 2000 K and possibly some early phase degradation. Among the topics of concern is the hydrogen generation due to contact between the overheated cladding and the flowing steam. Eighteen experiments have been carried out under a range of flooding/cooling conditions and pre reflood transient scenarios, thus creating an extensive database for model development and code improvement in the field of severe accident simulation. The experiments to date are summarised in Table 1.

One of the ultimate goals of QUENCH is to identify the limits (temperature, injection rate, etc.) for which successful reflood and quench can be achieved, and thus address one of the issues concerned with in vessel coolability during a Beyond Design Basis Accident (BDBA) (Birchley et al., 2010).

In some situations air ingress scenarios may occur: during a severe accident the reactor pressure vessel could fail and air could ingress; during mid loop operation when the reactor coolant system is open to the containment; in a spent fuel pool following loss of cooling or accidents during handling or transport accidents. The impact of air ingress on accident escalation has been the subject of numerous investigations in recent years, due to the twin effects of its components oxygen on heat generation and on the speciation of radiologically significant fission products, and nitrogen by degrading the effectiveness of the cladding oxide layer as an inhibitor of rapid oxidation and a barrier to fission product release. Integral experiments (IE) have been performed in several facilities: QUENCH (Steinbrück et al., 2006; Stuckert and Steinbrück, 2014), PARAMETER (Stuckert et al., 2016), CODEX (Hózer et al., 2002), and SFP (Adorni et al., 2016) to study the transient response during air ingress for representative geometries and conditions. In

Abbreviations: CP, Cathcart-Pawel; UH, Urbanic-Heidrick; Ls, Leistikow; PC, Prater-Courtright; SET, Separate Effects Test; IE, Integral Experiment; KIT, Karlsruhe Institute of Technology; (B)DBA, (Beyond) Design Basis Accident.

* Corresponding author.
E-mail address: birchley@hotmail.com (J.C. Birchley).

Table 1
QUENCH test matrix.

Test	Quench medium and injection rate	Temp. at onset of flooding	H_2 production before/during cooldown, g	Remarks, objectives
QUENCH-00	Water	≈1800 K		Commissioning tests
Oct. 9 - 16, 97	80 g/s			
QUENCH-01	Water	≈1830 K	36/3	COBE Project;
Febr 26, 98	52 g/s			partial fragmentation of pre-oxidized cladding
QUENCH-02	Water	≈2400 K	20/140	COBE Project; no additional pre-oxidation; quenching from high temperatures
July 7, 98	47 g/s			
QUENCH-03	Water	≈2350 K	18/120	No additional pre-oxidation, quenching from high temperatures
January 20, 99	40 g/s			
QUENCH-04	Steam	≈2160 K	10/2	Cool-down behavior of slightly pre-oxidized cladding by cold steam injection
June 30, 99	50 g/s			
QUENCH-05	Steam	≈2020 K	25/2	Cool-down behavior of pre-oxidized cladding by cold steam injection
March 29, 2000	48 g/s			
QUENCH-06	Water	≈2060 K	32/4	OECD-ISP 45; prediction of H_2 source term by different code systems
Dec 13 2000	42 g/s			
QUENCH-07	Steam	≈2100 K	66/120	COLOSS Project; impact of B_4C absorber rod failure on H_2, Co, CO_2, and CH_4 generation
July 25, 2001	15 g/s			
QUENCH-09	Steam	≈2100 K	60/400	As QUENCH-07, steam-starved conditions prior to cooldown
July 3, 2002	49 g/s			
QUENCH-08	Steam	≈2090 K	46/38	As QUENCH-07, no absorber rod
July 24, 2003	15 g/s			
QUENCH-10	Water	≈2200 K	48/5	LACOMERA Project;
July 21, 2004	50 g/s			Air ingress
QUENCH-11	Water	≈2040 K	9/132	LACOMERA Project;
Dec 08, 2005	18 g/s			Boil-off
QUENCH-12	Water	≈2100 K	34/24	ISTC Project No. 1648.2; VVER bundle with E110 claddings
Sept 27, 2006	48 g/s			
QUENCH-13	Water	≈1820 K	42/1	SARNET; impact of AgInCd absorber rod failure on aerosol generation
Nov 7, 2007	52 g/s			
QUENCH-14	Water	≈2100 K	34/6	ACM series: M5® cladding
July 2, 2008	41 g/s			
QUENCH-15	Water	≈2100 K	41/7	ACM series: ZIRLO™ cladding
May 27, 2009	48 g/s			
QUENCH-16	Water	≈1870 K	144/128	LACOMECO Project;
July 27, 2011	53 g/s			Air ingress
QUENCH-17	Water	≈1800 K	110/1	SARNET-2;
Jan 31, 2013	10 g/s			Debris formation and coolability
QUENCH-18	Water	≈1950 K	57/238	ALISA Project; air ingress
Sept. 27, 2017	53 g/s			AgInCd absorber rods

Table 2
Cases simulated.*

	Case
1	SCDAPSim/mod3.5/da/psi (CP/UH correlation; oxide breach at 2200 K, reduced injection + Ar flow due to shroud breach)
2	as (1) but breakaway and N_2 accelerated kinetics switched off
3	SCDAPSimlmod3.5/da/psi/lfm (as (1) but kinetics reduced at low [O_2])
4	as (3) but LS/PC steam correlation instead of CP/UH (Benchmark)
5	as (3) but no effect of shroud breach
6	as (3) but oxide breach at 2600 K to suppress melt relocation
7	as (3) but postulated steam inflow during reflood
8	as (4) but postulated steam inflow during reflood
	Data

* Results of cases displayed in groups over three phases and colour coded:
1, *4*, **data**: pre-oxidation (steam oxidation).
1, *2*, *3*, *4*, **data**: air/steam, reflood (air/steam oxidation).
5, *6*, *7*, *8*, **data**: reflood.

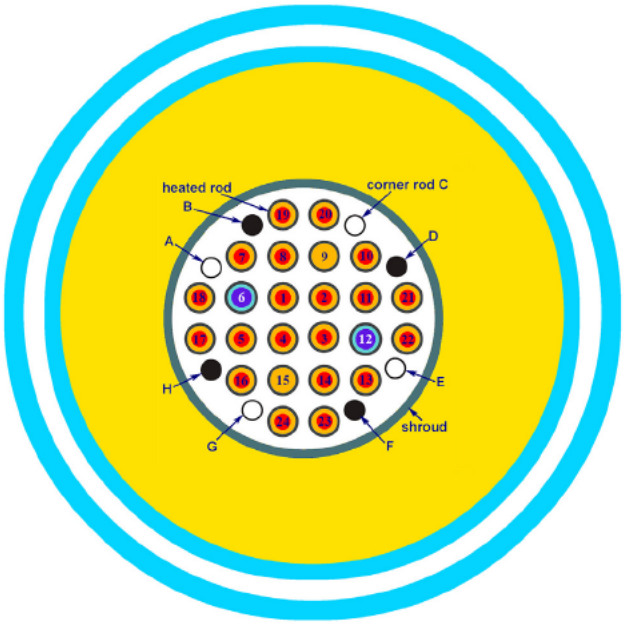

Fig. 1b. Cross section of QUENCH-18 bundle.

parallel, many separate effects tests (SET) have been performed under prescribed conditions to provide detailed data on the processes which control the reaction between cladding and the gas environment, for example, by KIT (Steinbrück, 2009; Steinbrück et al., 2017; Steinbrück and Schaffer, 2016) and IRSN [Duriez et al., 2008]. The SE and IE complement each other so as to provide an extensive database to address issues arising from air ingress.

Most of the previous experiments have concentrated on air as the reacting medium, often after a period of pre oxidation in steam or oxygen. The recent experiment QUENCH 18 (Stuckert et al., 2018) was conducted in the framework of the EU China project ALISA. It followed on from previous air ingress experiments QUENCH 10 (Steinbrück et al., 2006) and 16 (Stuckert and Steinbrück, 2014). The latter of these was followed closely during the initial stages of QUENCH 18, but for the first time a steam air mixture was used instead of air alone, constituting a more realistic simulation of a reactor or spent fuel accident. The test bundle included two unheated pressurised rods. There were also two

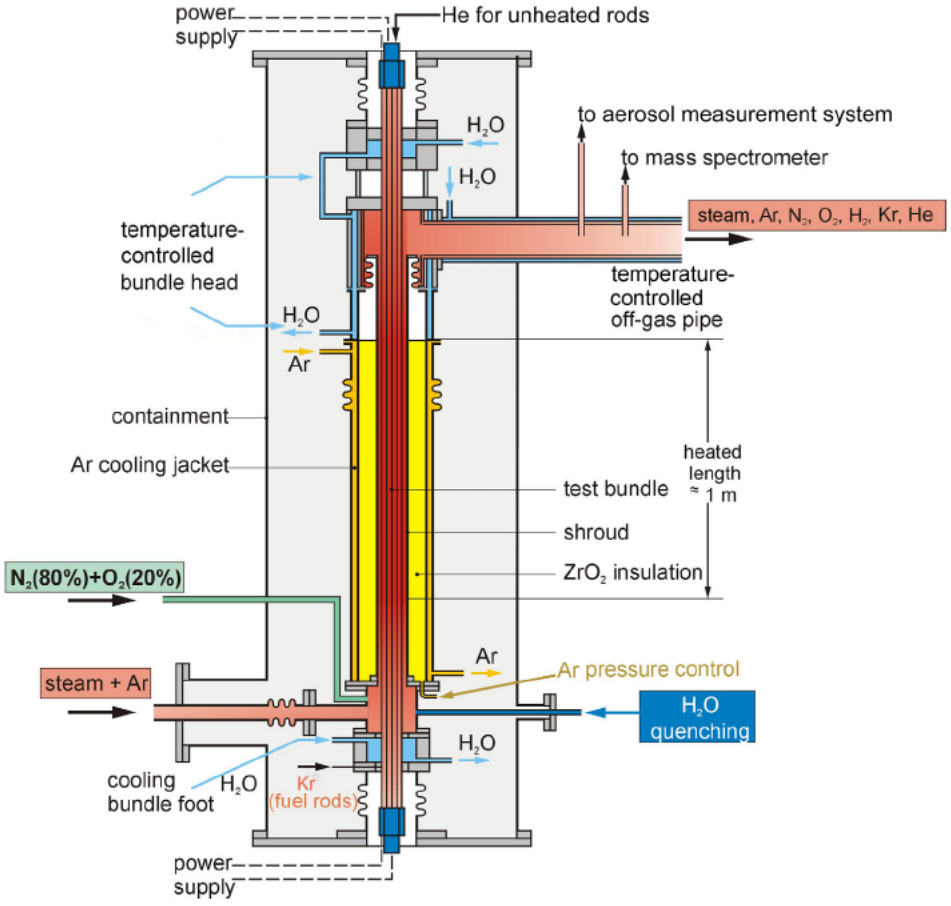

Fig. 1a. Schematic of QUENCH facility.

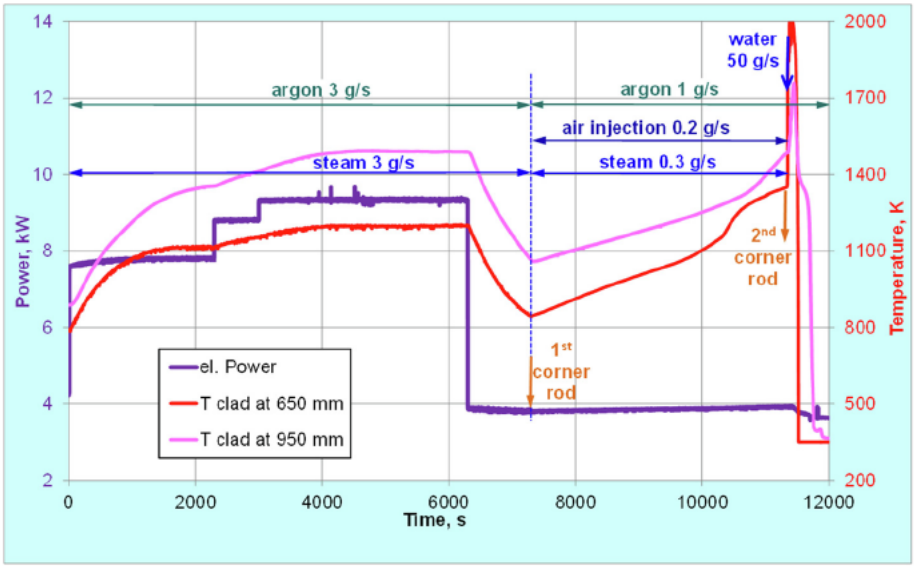

Fig. 2. Outline of QUENCH-18 test conduct.

Ag In Cd control rods, and reflood was therefore delayed until after the start of degradation in order to investigate the release of absor ber material.

2. Summary of QUENCH facility and test conduct

The QUENCH 18 bundle was configured in a cropped 6x6 array of rods about 2.5 m long, comprising 20 fuel rod rods electrically heated over a length of 1024 mm, 2 unheated rods, and 2 Ag In Cd absorber rods. The heating was by DC power delivered to 5 mm diameter tungsten elements in the rod centres which were surrounded by annular ZrO_2 pellets to simulate the UO_2 fuel. The geometry and most other bundle components are prototypical for Western type PWRs (M5® claddings and the AREVA AH 32715 grid spacers) while the rod radius and pitch were 9.5 mm and 12.6 mm, respectively, typical of a modern Westinghouse PWR. The heated rods were filled with helium at about 0.22 MPa at lab temperature, a slight overpressure relative to the test section (0.2 MPa) to allow rod failure detection by the mass spectrometer. The unheated rods were pressurised to 55 bar to investigate bal looning and burst. Eight Zircaloy 4 corner rods were installed to mount additional thermocouples. Two of the uninstrumented cor ner rods were withdrawn during the test to determine the axial oxidation profile at critical phases, while the others were examined after the test. The bundle was surrounded by a 3 mm thick Zr shroud to provide encasement, a 36 mm thick ZrO_2 fibre insulation, and a double walled stainless steel cooling jacket within which a flow of coolant is maintained to remove excess heat. The whole set up is enclosed in a steel containment. The test facility and bun dle cross section are shown schematically in Figs. 1a and 1b.

The test bundle, shroud, and cooling jacket are extensively equipped with thermocouples at different elevations and orienta tions. The test section incorporates pressure gauges, flow meters, and a water level detector. Hydrogen and other gases are analysed by a mass spectrometer at the off gas pipe about 2.7 m behind the test section.

The QUENCH 18 experiment conduct is indicated in Fig. 2: ini tial heat up, pre oxidation, transient, and quenching. During heat up the bundle reached a temperature of about 1400 K at the hot test elevations, 950 mm from the bottom of the heated section. A temperature plateau was maintained to provide the desired amount of cladding oxidation. A first corner rod was withdrawn near the end of this phase. The power was then reduced to allow a period cooling lasting ca. 1000 s in order to reduce temperatures to ca. 1100 K at which oxidation is insignificant. The electrical power was held constant at this reduced level until the end of the transient.

The air ingress phase was initiated by reducing the steam and argon flows to ca. 0.3 and 1 g/s respectively, and initiating air flow at 0.2 g/s. The reduced flow would allow the temperatures to increase to the point where oxidation recommenced, first by oxy gen and later by steam as well. The oxidation was accompanied by increased heating and subsequently by renewed hydrogen gen eration when the oxygen was fully consumed. This continued until sufficient absorber material was detected in the offgas line to pro vide useful data on the failure of the absorber rods and release of Ag In Cd. By this time the maximum temperatures were well in excess of 2000 K and bundle degradation had started. It was about this time that increased argon flow in the offgas line suggested a breach in the shroud.

A second corner rod was withdrawn and shortly afterwards the air, steam were terminated. The argon flow was switched from the lower to the upper volume. Reflood was then initiated. During reflood, water was injected at the bottom of the test section at 51 g/s, and power was reduced slightly to simulate typical decay heat level. The data for liquid level in the bundle and the exit flows strongly indicated that ca. 10 kg of water were spilled through the breach in the shroud over a period of 200 s or so during the early part of reflood. The spillage will certainly have slowed down the refill and quench progression and may also have influenced the oxidation excursion.

Following reflood initiation a major oxidation excursion occurred. Peak temperatures of ca 2500 K were estimated as all the thermocouple readings were affected in the hottest locations. Hydrogen production was 12.3 g in the pre oxidation phases, as planned very similar to QUENCH 16, and ca. 47 g in the air ingress phase. About 240 g hydrogen was generated during reflood. The remaining two corner rods were withdrawn after the test, again to check total oxide formation and hydrogen absorption.

3. Analytical tools used

3.1. Simulation code

SCDAPSim evolved from SCDAP/RELAP5/MOD3.2 (Siefken et al., 1997) which comprises a two fluid treatment of the thermal

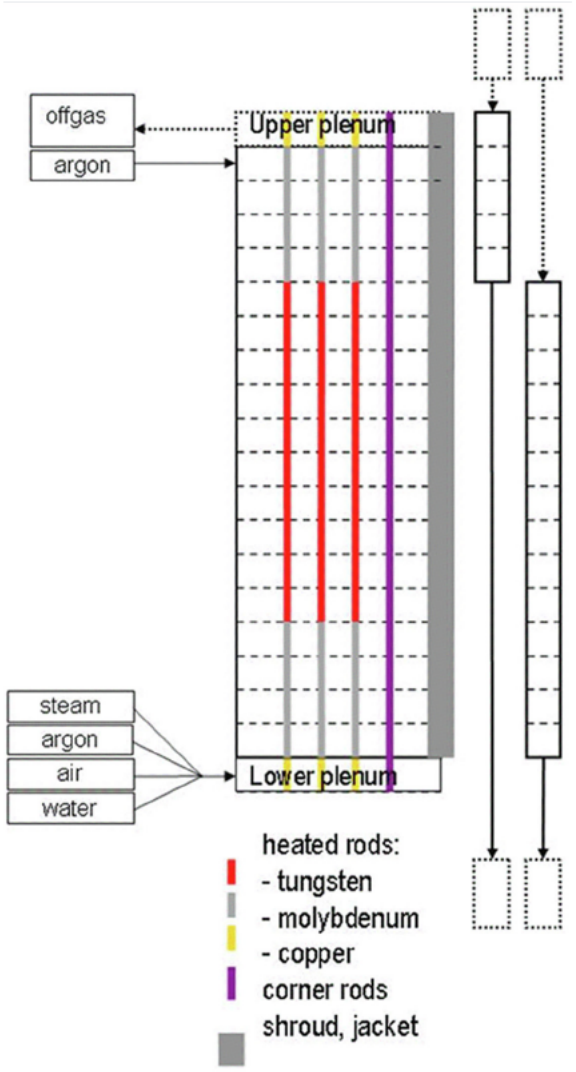

Fig. 3. SCDAPSim noding for QUENCH-18.

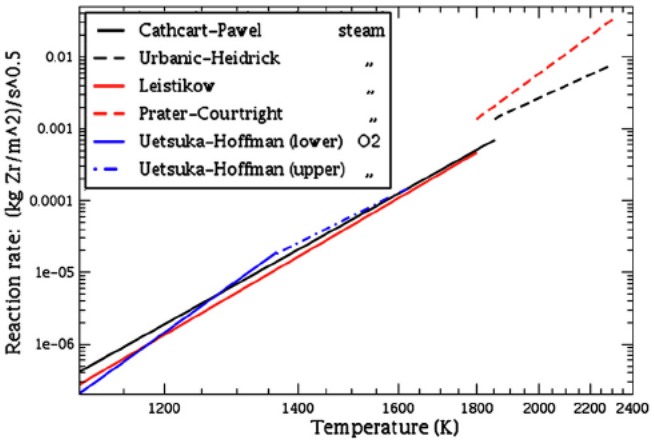

Fig. 4. Parabolic kinetic coefficients.

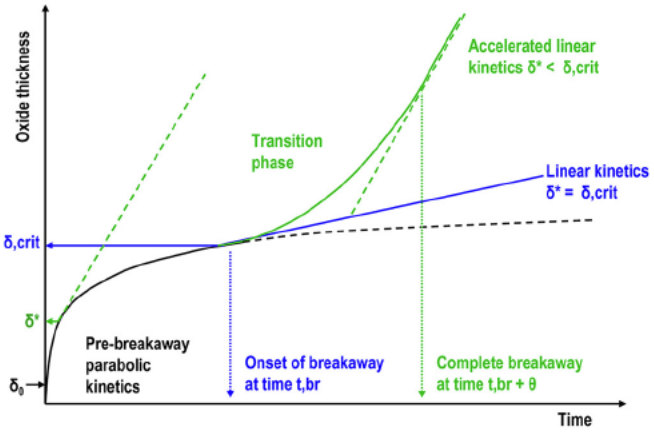

Fig. 5. Schematic of PSI model for accelerated (breakaway) oxidation.

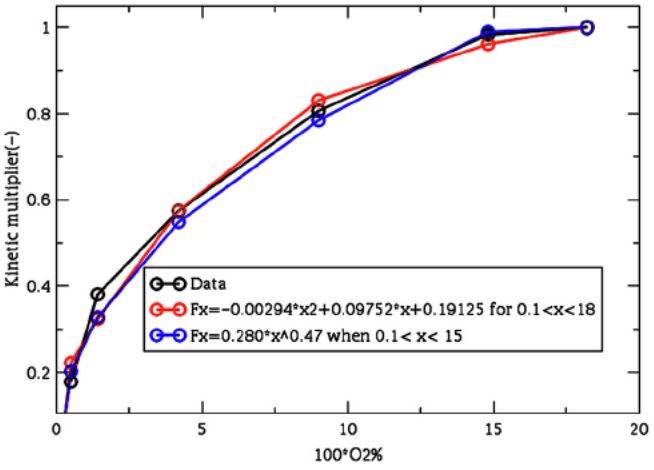

Fig. 6. Concentration dependent multiplier on rate coefficient oxidation by oxygen.

hydraulics and semi mechanistic modelling of the core degradation from its onset through to the late phase molten pool behaviour. Included in the core modelling are features to describe the QUENCH heater rods (Hering and Homann, 2007; Madokoro et al., 2015). The version used in the present analysis is SCDAPSim/mod35/da/psi which contains the PSI developed air oxidation model (Birchley and Fernandez Moguel, 2012; Fernandez Moguel and Birchley, 2012). It is identical to the version mod3.5/da released by ISS in 2009. The psi variant includes additional options for the catalysing effect of nitrogen. Calculations were also performed with a local version in which the oxygen consumption rate is modified to take account of oxygen concentration.

The input model is based on the one used in analyses of the previous QUENCH experiments, starting with QUENCH 06 (Sepold et al., 2004; Hering et al., 2002) which was subject of CSNI International Standard Problem 45. The present model was evolved directly from the model used in the QUENCH 16 analysis (Fernandez Moguel and Birchley, 2013) to reflect the change in bundle configuration and the inclusion of the two absorber and two unheated pressurised rods. This was the model used for the pre test prediction (Hollands, 2017). The starting point for the model used in the present post test analysis is identical, but with the actual boundary conditions applied.

The model is shown schematically as the noding diagram in Fig. 3 comprises a single radial and eighteen axial hydraulic nodes for the test section with ten nodes for the 1 m tungsten heated length. The cooling jackets are represented by separate hydraulic systems and containment is represented as a boundary condition. Although the number of axial nodes comparable with many plant models, the node length is shorter, as dictated by the need to resolve the steep temperature profile in QUENCH.

A point about QUENCH is the significant fraction of total electri cal power that is dissipated by the electrical resistance of the exter nal circuitry and its contact with the copper electrodes; the same value of 3.6 mΩ/rod is used as in the pre test analysis.

3.2. Choice of oxidation models

It is known that the hydrogen generation and likelihood of an excursion during reflood can depend strongly on the choice of oxi dation correlation. The SCDAPSim default model is the pairing Cathcart Pawel (CP) (Pawel et al., 1979) and Urbanic Heidrick (UH) (Urbanic and Heidrick, 1978) correlations for oxidation in the temperature regimes below 1853 K (low/intermediate) and above 1873 K (high), with linear interpolation in between. The combination is part of the MATPRO material property library (vol ume 4 of the SCDAP/RELAP5 manual). The present code version allows additional options, including the Leistikow (Ls)/Prater Courtright (PC) (Schanz et al., 2004) pair of correlations for the lower and high temperatures, respectively, which was used to examine sensitivity to steam oxidation kinetics. The Uetsuka Hoffman correlation (Uetsuka and Hofmann, 1985) was used for the oxygen oxidation rate. As can be seen from the comparison in Fig. 3, the Ls/PC choice gives slower oxidation at the lower tem peratures but faster at high temperatures. The Uetsuka Hofmann kinetics is comparable with Leistikow. All these correlations assumed parabolic kinetics. The temperature dependent coeffi cients are shown in Fig. 4.

The above mentioned model for accelerated oxidation due to nitrogen is similar to the model for breakaway in steam (or oxygen), i.e. a transition from parabolic to linear kinetics is trig gered when the oxide layer reaches a critical thickness, δ,crit. It is applied in the presence of nitrogen with either (or both) oxygen and steam, and the post transition state persists even after the end of the air phase. The model is indicated schematically in Fig. 5 and is described in (Birchley and Fernandez Moguel, 2012). Different parameter values for δ,crit are used with and without nitrogen present.

In connection with oxidation by oxygen, several of the simula tions were performed with a concentration dependent reduction factor (Vryashkova et al., 2013) applied to the rate coefficient, Fig. 6. This was derived from thermo gravimetric SETs performed at KIT (Steinbrück et al., 2011) for a range of air argon mixture ratios which showed reduced kinetics at low oxygen concentration.

The reduction factor is a function of oxygen concentration and is applied in addition to the acceleration due to nitrogen. It takes the value 1.0 for oxidation in air at and near its normal composi tion, and decreases as the oxygen is progressively consumed. The value also decreases if any non reacting gas such as argon is added. The data (Steinbrück et al., 2011) were obtained from tests with air argon mixtures so the factor does not take account of how the kinetics might be influenced by a reactive species such as steam even though it is not being consumed locally.

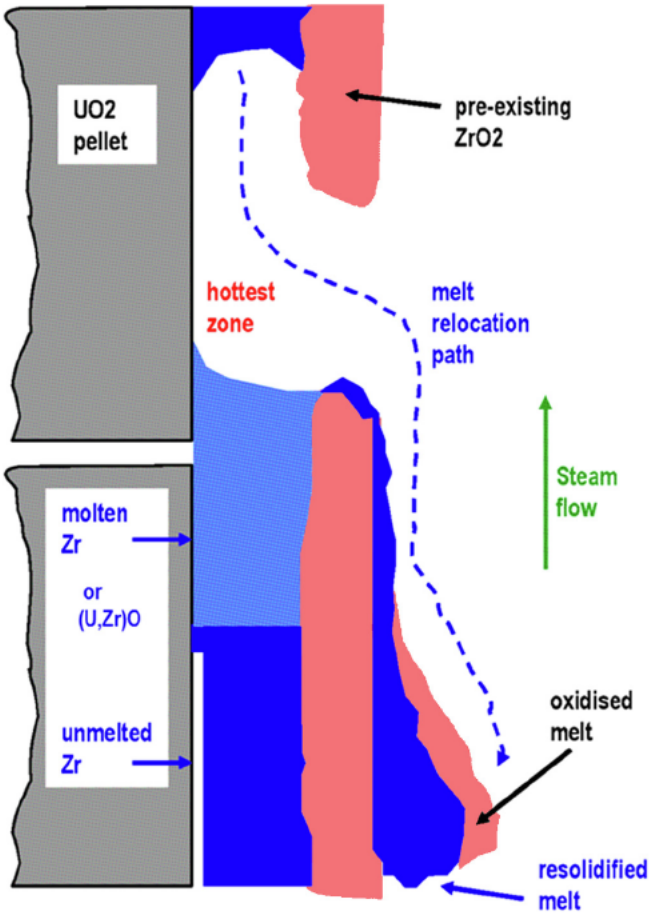

Fig. 7. Melt relocation and oxidation model in SCDAPSim.

3.3. Choice of metallic melt relocation criterion

Experimental programmes on reflood from high temperature have shown that the injection of coolant does not always lead to immediate cooling. In some cases there was a significant tempera ture excursion, as a result of rapid oxidation of the cladding, e.g. QUENCH 02, 03, 07 and 09, (Hofmann et al., 2000; Steinbrück et al., 2004a, 2004b) as well as QUENCH 16 and PARAMETER SF4 (Stuckert and Steinbrück, 2014; Stuckert et al., 2016). A strong excursion was typically observed if degradation had already started or if the oxide layer had been weakened following oxidant starvation or due to the effect of nitrogen, causing unoxidised metallic material to be exposed to the steam flow. SCDAPSim includes a simple phenomenological model for rapid oxidation of molten metallic that is released following a breach of the oxide layer. An oxide layer forms on the molten metallic but is breached again, so the unoxidised surface may be repeatedly renewed, as indicated schematically in Fig. 7. The occurrence of breach of the oxide layer is essentially determined by a user specified tempera ture criterion which can take any value in the interval from 2200 K which is somewhat above the metallic melting temperature, to 2600 K which is somewhat below the oxide melting temperature.

4. Post-test simulations of QUENCH-18

4.1. Cases simulated

A total post test of eight calculations are performed. The same pre test analyses input model, but with the experimental bound ary conditions for electrical power and inlet flows as functions of time, was used for the initial calculation. The main difference between the pre and post test calculations was that QUENCH 18 was originally planned with reflood from ca. 1800 K in attempt to avoid bundle degradation or excursion. Up to that point the planned and actual boundary conditions were very similar. How ever, it was later decided to continue the air ingress phase to study the release and aerosol transport of absorber material following failure of the control rods. This led to long periods of oxygen and steam starvation and also much higher temperatures at the start of reflood. The changed protocol means that there is no basis for

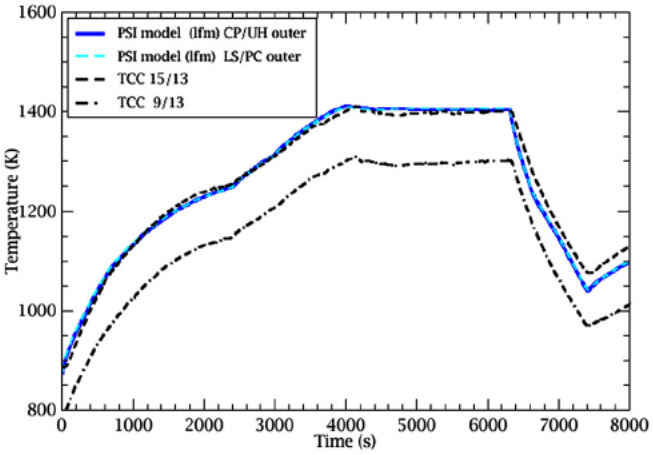

Fig. 8. Comparison for centreline temperatures at 950 mm during preoxidation (cases 1, 3).

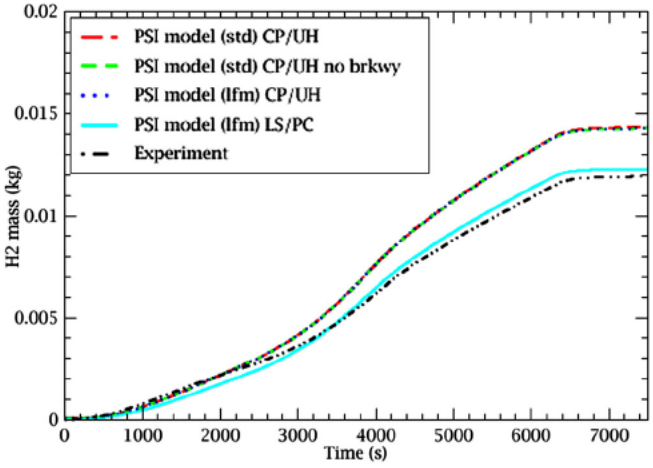

Fig. 9. Comparison for H_2 generated during preoxidation (cases 1, 2, 3, 4).

useful comparison of the pre test calculated outcome with that of either the post test or experiment itself.

Due to the shroud breach, the effective boundary conditions dif fer from those applied by the experimenters. The initial input does not take account of the breach and so cannot be regarded as a true base case. However, it provides a useful starting point for develop ing a best estimate case and exploring the observed behaviour by means of sensitivity studies. The various cases are identified in Table 2.

The experiment is analysed via comparisons between experi ment and calculations in the three main phases: preoxidation, air ingress, reflood.

During preoxidation and air ingress, four simulations (cases 1, 2, 3, 4 in Table 2) were performed, differing only as regards oxidation kinetics. For steam oxidation CP/UH is used in cases 1, 2, 3 and Ls/ PC in case 4. Case 1 uses the PSI model breakaway for both steam and air oxidation, but it is disabled in case 2. Breakaway is retained in cases 3, 4 but a reduction factor is applied to oxidation kinetics at low oxygen concentration. Thus 1, 3 are identical except for oxy gen oxidation kinetics, whereas 3 and 4 are identical apart for steam oxidation correlation.

4.2. Analysis of preoxidation (0 7410 s)

During this and the other phases of QUENCH 18, the unheated rod centreline temperatures are used for code comparison with

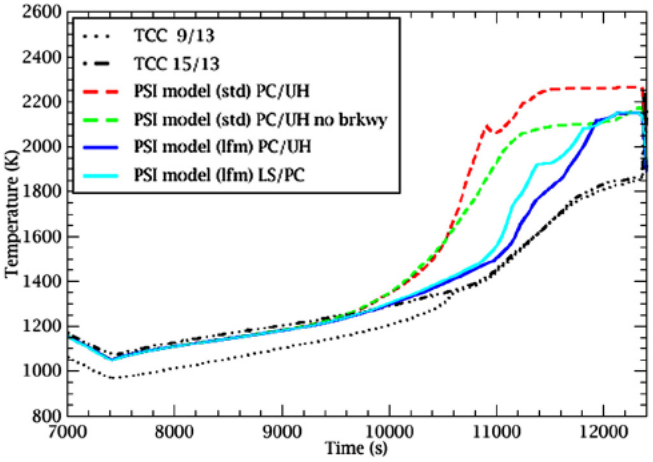

Fig. 10. Comparison for centreline temperatures at 950 mm during air ingress (cases 1, 2, 3, 4).

experiment, as they provided meaningful data until well into reflood.

Fig. 8 shows the choice of oxidation correlation (cases 3, 4) makes only very slight difference to the temperature at the hottest location, centreline of the two unheated rods at 950 mm. This is to be expected as the oxidation heat is a small fraction of the total during preoxidation. There is remarkably good agreement for the measured temperature on rod 16 but a consistent overestimate by ca. 100 K on rod 9 despite the two rods being nominally the same.

There is a moderate difference in hydrogen generation between the correlations as seen from Fig. 9, but with excellent agreement when Ls/PC is used. Disabling the breakaway model (case 2) in the CP/UH case makes no discernible difference to the hydrogen gener ation, despite transition to breakaway being initiated (cases 1, 3) at some locations shortly before the end of preoxidation. The modifi cation to oxygen kinetics also makes no difference during this phase, but is included as verification of the special code version (. . ../da/psi/lfm).

At first sight the results suggest the Ls correlation is to be pre ferred over CP, and in fact it probably better reflects the slower pre breakaway kinetics in the monoclinic ZrO_2 regime below about 1300 K. However, only one elevation is used in the temperature comparison and the good agreement for TCC 15/13 is not

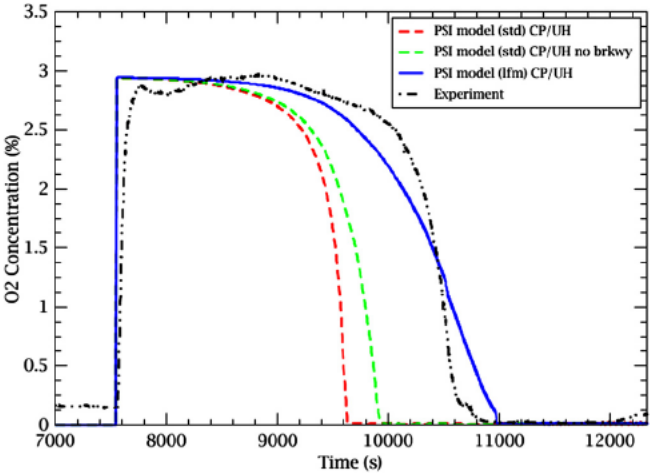

Fig. 11. Comparison for O_2 concentration at bundle exit during air ingress (cases 1, 2, 3).

replicated across the bundle as a whole. For the analysis of the air ingress phase, it is beneficial to begin with as good agreement as possible of the total oxidation.

4.3. Analysis of air ingress phase (7410 12,330 s)

The same four simulations are compared with experiment in this phase as above. However, unlike preoxidation, the modelling of air oxidation now has strong bearing on the results. Comparison is again made for the unheated rod centreline temperatures at 950 mm, shown in Fig. 10.

Following the reduction in steam and Ar flow to 0.3 and 1 g/s, respectively, the temperature starts to increase after previously having dropped. During the next about 2500 s the increase is very gradual in the absence of significant oxidation heat, with the calcu lations almost coincident and closely following the observed increase. The temperatures calculated in cases 1 and 2 then increase more rapidly, departing from the data which show a later and milder increase in slope. The difference between those case is due to breakaway (strictly, nitrogen induced acceleration) being disabled in case 2. Cases 3 and 4 continue to follow the data for several hundred seconds before increasing more sharply than in the experiment. The improved agreement is due to the slower oxi dation at low oxygen concentration. Despite some improvement in cases 3 and 4, the temperatures at the end of this phase are over estimated by about 300 K. Curiously, the two centreline measure ment almost coincide after the TCC 9/13 reading increase at about 10500 s. It is natural to ask if the measurement was offset low until then.

The simulated (CP/UH steam kinetics) and experimental oxygen concentrations at the bundle exit are compared in Fig. 11. In the experiment and all the calculations the complete oxygen consump tion coincides with the faster increase in temperature, when steam consumption recommences. This occurs earliest in case 1 and lat est in case 3. Although case 3 (reduction factor at low oxygen con centration) gives the best agreement for the time of complete consumption, that may be fortuitous since the consumption rate is underestimated at concentrations below about 2%.

As might be expected, the onset of hydrogen generation imme diately follows the time of complete oxygen consumption in both the experiment and simulations, as shown in Fig. 12. The calcu lated temperature rise rate (recalling Fig. 10) is then roughly inde pendent of the air oxidation modelling, as may be expected as it is essentially determined by the steam flow rate.

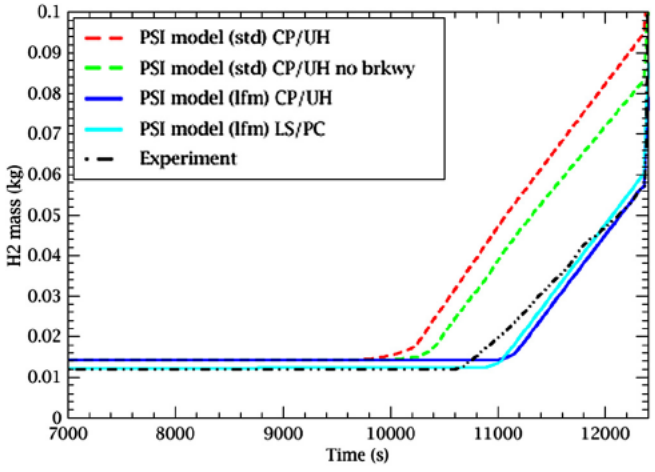

Fig. 12. Comparison for H_2 generation during air ingress (cases 1, 2, 3, 4).

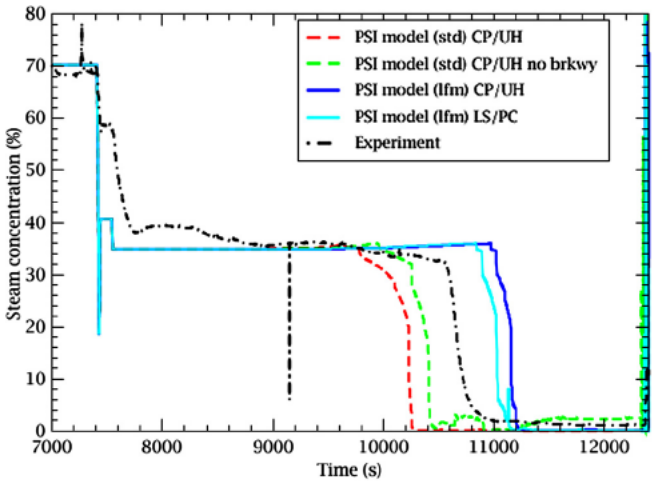

Fig. 13. Comparison for steam concentration at bundle exit during air ingress (cases 1, 2, 3, 4).

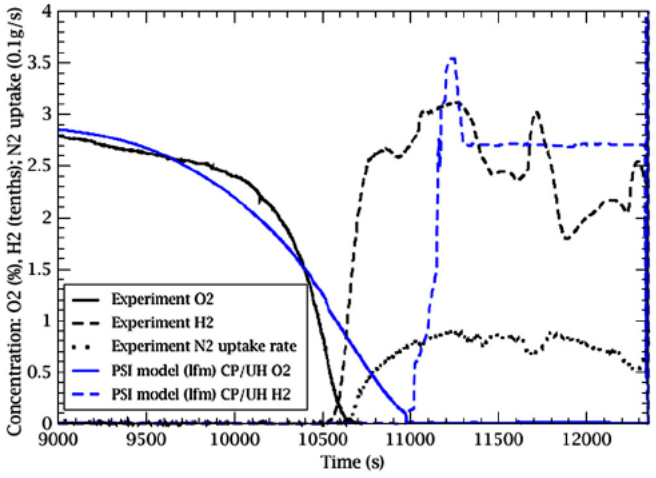

Fig. 14. Comparison for H_2 and O_2 concentration at bundle exit during air ingress (case 3) with experimental N_2 flow rate.

The calculated generation increases quickly to a rate corre sponding to complete steam consumption, i.e. 0.034 g/s in each case. However the observed hydrogen release, average 0.027 g/s, corresponds to roughly 80% in contradiction to the offgas pipe measurement which suggests almost complete steam consump tion, as seen from Fig. 13. One might suppose the discrepancy is due to measurement uncertainty, but it is worth asking if some of the hydrogen might have been absorbed in the cladding previ ous experiments at KIT suggest this can occur during breakaway oxidation or when the oxide layer is otherwise damaged (Große et al., 2009; Grosse et al., 2018a, 2018b).

Of the four cases, 1 and 2 use the standard PSI model for air oxi dation and give rapid oxygen consumption and hence early onset of hydrogen generation, even if breakaway is disabled. These cases also significantly overestimate the extent of oxidation at reflood initiation and are therefore not ideal for continuing the analysis. Cases 3 and 4 include the reduction factor at low oxygen concen tration and give close agreement for the total pre reflood oxida tion. However, the good agreement is rather fortuitous since the later than observed onset of hydrogen production and the faster than observed rate almost exactly cancel out. Although the true oxidation might have been more than as indicated by measure ment, case 3 (CP/UH steam and modified oxygen kinetics), is regarded as the revised base case in preference over case 1.

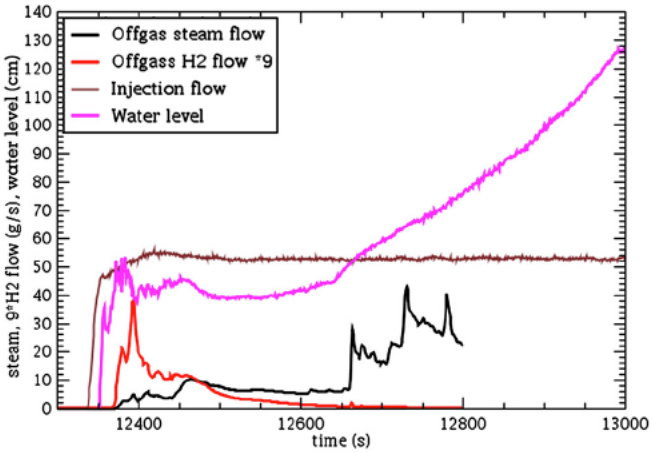

Fig. 15. Observed offgas steam and H_2 flow, water level and injection rate.

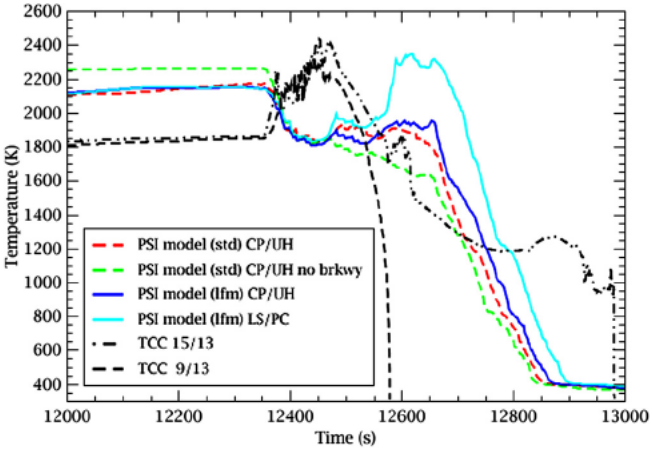

Fig. 16. Comparison for centreline temperatures during reflood (cases 1, 2, 3, 4 – effect of oxidation models).

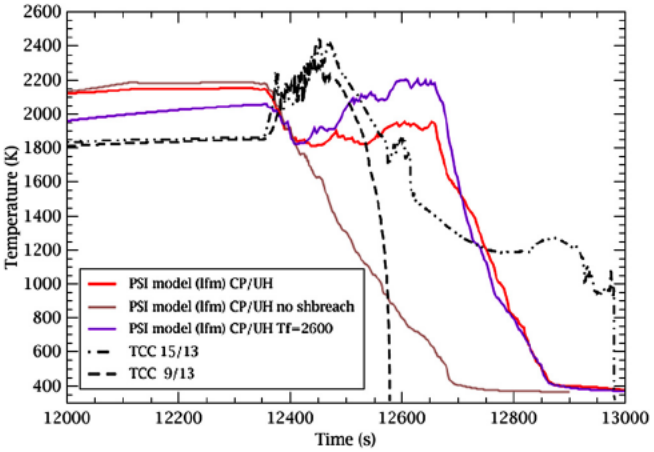

Fig. 17. Comparison for centreline temperatures during reflood (cases 3, 5, 6 – effect of bundle assumptions).

As seen from Fig. 14, the simulations show a clean switch from complete oxygen consumption to hydrogen release with no period of overlap. The calculated behaviour is implied by the single channel input in conjunction with the code model exclusion of oxygen and steam being consumed simultaneously and locally. By contrast the experiment shows a minor overlap, possibly due to variations in oxygen concentration across the bundle. Although any hydrogen thus produced would be expected to recombine with residual oxygen, the flow might not have been sufficiently mixed for that to have happened when the starvation was local. The data also show uptake of between 0.05 and 0.1 g/s nitrogen starting very shortly before the onset of steam starvation. It would seem that the uptake is prevented by the presence of steam, and that the small overlap in timing might be due to local starvation. The uptake begins before complete steam starvation but does not reach its maximum value until all the steam is consumed. However, it is not clear if the presence of steam and nitrogen uptake affect each other's reaction with the cladding. It may be that the uptake increased together with the extent of the oxygen starved region. SCDAPSim does not contain any model for Zr nitrogen reactions so cannot shed any light.

4.4. Analysis of reflood

The reflood behaviour is analysed by means of two sets of modelling studies. Cases 1, 2, 3 and 4 that were used to analyse the pre reflood oxidation are also used to study the effect of oxidation models on reflood. Cases 5, 6, 7 and 8 involve different assumptions concerning the bundle and the reflood boundary conditions.

The key signatures observed during reflood are the collapsed water level in the bundle and the flows of steam and gases in the offgas line, shown in Fig. 15. Most of the high temperature readings are compromised by the damage to shroud and cladding, but the unheated rod centreline temperatures proved comparatively robust and are used in the comparison with simulations.

We first consider the observed signatures alone. The rapid filling of the lower volume and initiation of reflood resulted in a rapid increase in water level to almost 500 mm, after which the level increase stalled for about 250 s. Measured additional argon flow indicate the shroud breached about 1100 s before reflood, thought by the experimenters to have been between 200 and 500 mm based on to observations. The level measurement suggests the breach might have been between 400 and 500 mm. The experimenters also estimate that about 10 kg of water spilled into the space behind the shroud which is consistent with a large fraction, 40 g/s, of the injected water being spilled during the 250 s when the level was not rising. It is not thought useful to attempt to model the spillage; instead the base case assumes an injection rate reduced from the nominal 52 g/s to 12 g/s during 12,390 to 12,640 s. In addition an argon flow of 0.6 g/s into the bundle at 450 mm is assumed starting at 11250 s, the time of breach. A case without these modifications is simulated as a sensitivity study.

The offgas steam and hydrogen flows also support this scenario. Until 12,650 s the steam flow is between 5 and 10 g/s before increasing again to more than 20 g/s. However, there was a large and rapid hydrogen release immediately after the initial level rise with a maximum corresponding to consumption of nearly 40 g/s steam. This implies a lot of contact between injected water/steam and hot material early during the reflood, although it is not clear what caused it. The effect of a large steam surge is subject of sensitivity studies.

Sensitivity study is also performed regarding the temperature criterion for breach of the oxide layer, resulting in breakout and relocation of molten Zircaloy. As previously mentioned, some of the experiments in QUENCH and other programmes exhibited excursions when reflood was initiated at maximum temperatures above the melting point, i.e. about 2100 K or more, and also at lower temperatures if the oxide scale had been degraded by some process such as starvation or exposure to air. SCDAPSim contains a model for rapid oxidation of exposed metallic melt, which is able to capture, at least qualitatively, the resulting excursion. On the basis

of these observations, 2200 K is adopted as the oxide breach criteria as the base case assumption to allow simulation of metallic relocation, while 2500 K is used in a sensitivity case to prevent relocation.

We first compare the same measured rod temperatures as before with the simulations, focussing separately on the effect of oxidation model (Fig. 16) and bundle assumptions (Fig. 17). All the simulations overestimate the temperature at reflood initiation, then cooling over the next 100 s which contrasts with the data which shows a large (+500 K) increase in this same timeframe that is consistent with the observed hydrogen release. All the cases using the default CP/UH oxidation kinetics show a similar behaviour, with no further increase in temperature at this location and steady cooling/quench after the full injection rate is restore after 12,640 s. The no breakaway (case 2) gives the most cooling, while the modified oxygen oxidation kinetics (case 3) gives slightly later onset of cooling, possibly because less of the cladding was already oxidised. Use of Ls/PC oxidation kinetics (case 4) departs from CP/UH during the period of reduced injection, with a significantly higher temperatures and slightly later cooling. Although the maximum temperature is close to the maximum measured, the temporal trends are very different. Data for rod 16 show the temperature remained higher for a longer period, very possibly because of blockages which were not simulated by the code. However, meaningful data are unavailable after 12,570 s for the rod 9 temperature.

The effects of temperature criterion for oxide breach and of injection rate are now separately compared with the base case.

With the nominal reflood (no shroud breach, case 5) steady cooling continues throughout the reflood resulting in much earlier quenching. In view of this and other signature comparisons (discussed elsewhere), the nominal reflood conditions and intact shroud is completely unrealistic.

Comparison of the increased oxide scale breach temperature (2500 K, case 6) with the base (2200 K, case 3) reveals a somewhat different signature, with a higher temperature during the period of reduced injection but then the same cooling trend as the base case. It should be mentioned that the relative temperatures at these locations are not necessarily indicative of those at other elevations, particularly as the bundle damage state is affected by the change in criterion from 2200 to 2500 K. The higher temperature criterion causes hot material to remain at the upper locations instead of relocating downwards.

Fig. 18 shows the results of a further sensitivity study, in which an additional flow of 1800 g steam from the breach into the bundle is arbitrarily assumed during the early part of reflood, peaking at 30 g/s at 12365 s and then decreasing, intended to correspond to the observed hydrogen flow. The objective is to examine how such a steam surge might have affected the temperatures and oxidation, without addressing the cause. However, a steam flow of this order of magnitude must have occurred in order to enable such a large generation of hydrogen. One possibility is that molten metallic or hot debris material relocated to the bottom of the test section; alternatively, or perhaps additionally, the early rapid refilling cause water to spill into through the breach and interact with hot material behind the shroud.

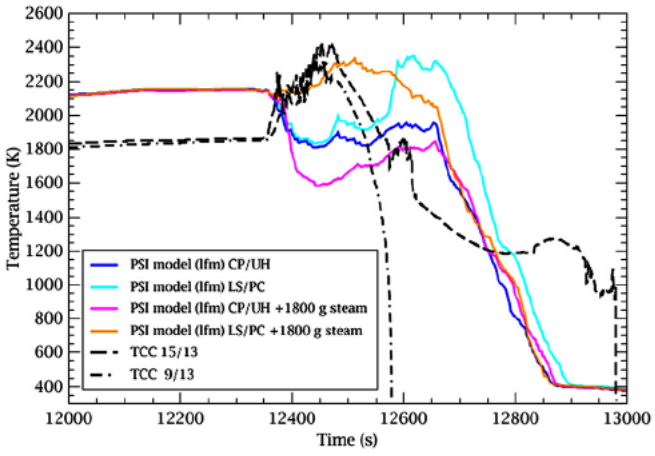

Fig. 18. Comparison for centreline temperatures during reflood (cases 3, 4, 7, 8 – effect of steam oxidation model with early added steam).

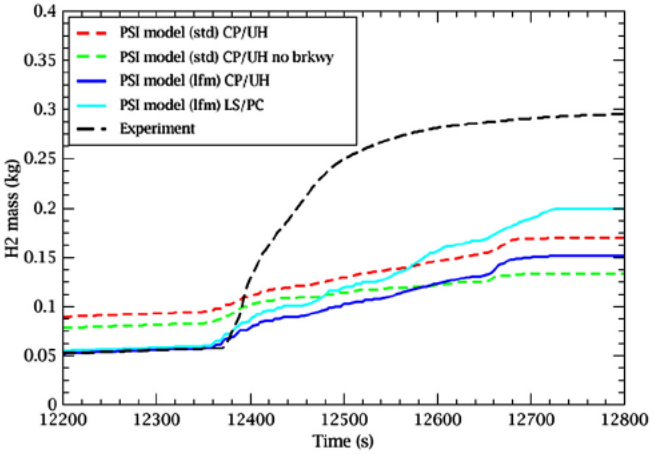

Fig. 19. Comparison for H_2 generation during reflood (cases 3, 4, 5, 6 – effect of oxidations models).

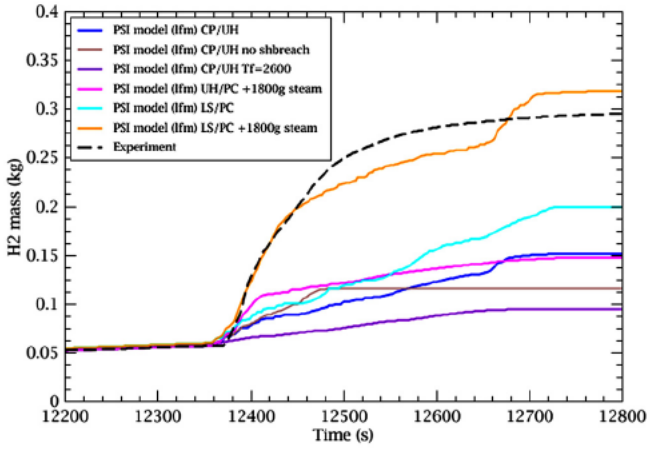

Fig. 20. Comparison for H_2 generation during reflood (cases 3, 4, 5, 6, 7, 8 – effect of bundle assumptions, added steam, and steam oxidation correlation).

With CP/UH kinetics (case 7) the additional steam simply increased the cooling during this period without any indication of additional heat generation. Contrastingly, Ls/PC (case 8) produces a temperature increase qualitatively similar to the observed response. Interestingly, the temperature traces come together later on when cooling is re established. This surprisingly large difference between these simulations points to a possible cliff edge effect regarding the effect of steam flow as a coolant and as a driver for oxidation.

Figs. 19 and 20 compare the calculated hydrogen generation with experiment for the different oxidation models and treatment of the bundle conditions, respectively, thus corresponding to the same cases as shown in Fig. 16 and Fig. 17/18. The production during reflood is indicated.

Use of CP/UH kinetics and the standard treatment of oxygen oxidation leads to a moderate increment in hydrogen mass, 75/51 g with breakaway enabled/disabled (case 1 and 2), respec tively. The accelerated oxidation due to nitrogen persists after the end of air ingress. The reduced kinetics at low oxygen concen tration (base case 3) results in a larger generation during reflood (96 g), possibly because less of the cladding has been previously oxidised. The agreement for starting value means a better basis for comparison with data. Use of Ls/PC (case 4) gives a yet larger amount (140 g) as may be expected due to the significantly faster PC kinetics at high temperature. None of these simulations capture the large generation during the first 100 s.

Comparison of cases 5 and 6 with 3, case 7 with 3, and case 8 with 4, reveals an even larger spread of values. The nominal injection (case 5), corresponding to no shroud breach, enhances the cooling with an earlier end to the oxidation and less hydrogen (59 g) than in the base case (96 g), despite more rapid generation (due to more steam flow) for part of the refill. There is some indication of steam starvation in the cases of reduced injection. With no metallic reloca tion (case 6) there is only 36 g hydrogen during reflood, demonstrat ing the strong effect of melt oxidation. The inclusion of additional steam flow (case 7) results in faster generation during the first 50 s but the total mass (92 g) is almost the same as the base case. All the above cases adopt CP/UH kinetics for steam oxidation.

The most striking comparison is between the two cases (4 and 8) using Ls/PC kinetics. With the additional steam flow the hydro gen mass increases from 140 to 239 g, in stark contrast to the close similarity between cases 3 and 7. In fact the production rate agrees remarkably well with the data during the early part of reflood and also rather well with the total. The level of agreement must obvi ously be regarded as fortuitous and should not be considered as indicating excellent modelling. However, the results suggest that a strong steam surge occurred during the early stage of reflood and had a major impact on the excursion. The results also support the view that metallic melt relocation occurs at temperatures not much higher than the melting point if the oxide scale is weakened, and that it strongly promotes an excursion. It may be argued on the basis of the present analysis that Ls/PC is an improvement over CP/ UH, or at least PC over UH, but it is less clear whether that would apply generally.

Fig. 21 compares the collapsed water level in the bundle for all the simulations with the measurement. There are discrepancies between the data and all of the simulations, most notably with the nominal injection (case 5) which does not exhibit any stalling of the level increase, not even much slowing. All the other cases are fairly similar, surprisingly so in view of the large differences in oxi dation. There is no very obvious correlation between magnitude of the excursion and level, except that the level calculated in cases 7 and 8, i.e. additional steam, are lower during the period of flow. It is likely that the steam flow entrained more water out of the test sec tion. The significant extra generation of hydrogen and hence heat in case 8 would also necessitate more water to be boiled off.

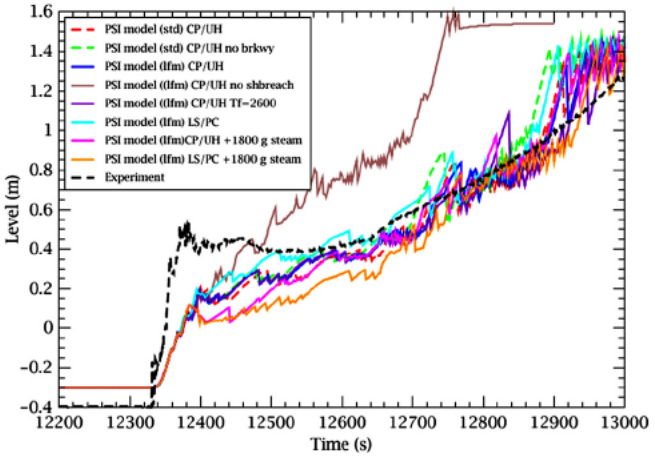

Fig. 21. Comparison for water level with all cases.

A possible reason for the similarity for water level between most of the cases, despite large differences in the other signatures, is that oxidic melting does not occur in these simulations. The SCDAPSim models do not calculate the full effect of metallic melt relocation and refreezing on channel blockage; therefore the calculated reflood progression is not directly impacted by the damage state.

None of the cases show the observed strong initial increase in level, and it was not possible to reproduce this behaviour with any credible injection rate. It is conjectured that prior damage to the bundle and shroud might have been more severe than envi sioned in any of the simulations. Possibly there was extensive relo cation of debris from damaged heater rods or from the shroud/ insulation to the lower part of the test section. If that were the case then the level rise would be greater, and there would also be a pos sibility of rapid boiling of water in contact with hot material. Another factor may be that the level measurement is based on dif ferential pressure whereas the calculated results show the col lapsed level itself. A large dynamic pressure drop would have increased the level deduced from pressure difference.

5. Discussion of phenomena and modelling

5.1. Preoxidation

The thermal hydraulic conditions during preoxidation were similar to earlier air ingress experiments, the only (minor) differ ence being the makeup of the bundle which is represented in the model. The thermal response at 950 mm is therefore well simu lated during both the heatup and cooldown periods, which is to be expected in light of extensive analyses of previous QUENCH experiments. The gross oxidation temporal trend was also very well simulated using both the default CP and Ls correlations, despite a modest quantitative overprediction with CP. The cause is possibly not the correlation but that the surface temperatures elsewhere in the bundle may have been overpredicted to some extent. Because of instrument uncertainty, and also the fin cooling effect of the externally attached thermocouples (which disturb the flow such as to increase the local heat transfer), the true tempera tures may have been higher than measured. It is noted that the centreline temperature readings TCC 15/13 and 9/13 tended to be higher than the cladding temperature at the same elevation on other rods.

Questions remain about the oxidation correlations at tempera tures below about 1300 K. Both correlation extrapolate the para bolic kinetics back from the range of key interest for Design Basis Accidents (DBAs), ca. 1500 K, and do not take account of the differ ent oxide morphology at the lower temperature where the (pre breakaway) kinetics are approximately cubic. Leistikow has stee per temperature dependence and hence goes some way to captur ing the behaviour, at least macroscopically. Among other correlation sets, Leistikow/Schanz (Leistikow et al., 1983) and Grosse (Grosse, 2010) include a separate branch applied in the lower range. However, the model with either correlation gives sat isfactory representation of the preoxidation overall, with Leistikow perhaps preferred.

5.2. Air ingress phase

Following the change in flow and gas composition, the temper atures increased due to the reduced heat transfer alone. Again the

thermal response at 950 mm is well simulated during the first ca. 2000 s of this phase when oxidation heat remained insignificant. It should be mentioned that the reduced flow cause the location of maximum temperature to shift downwards from 950 mm to 750 850 mm.

The temperatures increased more quickly as the oxygen began to be consumed, and these changes occur more rapidly in the sim ulations than was observed. A possible reason for the discrepancy might be that the accelerated oxidation due to the presence of nitrogen is over represented by the PSI model. However, it is not possible to make this a definite conclusion since the temperatures at locations below 950 mm, i.e. those which are now the hottest, appear to be overestimated in the simulation.

The overestimate of oxygen consumption rate is most marked when the PSI accelerated kinetics are applied in its standard form i.e. no reduction to take account of low oxygen concentration). However, even with the acceleration disabled the oxygen is still consumed more rapidly than observed. The acceleration is the result of a nitrogen induced degradation of the oxide layer integ rity, therefore allowing the oxygen to pass more readily to the underlying metallic. The degraded state of the oxide would persist even after nitrogen is no longer present, and therefore impact any subsequent oxidation.

Retaining the accelerated kinetics but applying the reduction factor gives better agreement for the time of total consumption. However, the onset is still earlier than observed while the rate becomes slower as total consumption is approached. The use of a reduction for low oxygen concentration seems justifiable in an air (+argon) environment but may be incorrect if steam is also pre sent to react with the cladding, whereupon the hydrogen produced can in turn react with residual oxygen, thus:

$$Zr + 2H_2O \rightarrow ZrO_2 + 2H_2,$$

$$2H_2 + O_2 \rightarrow 2H_2O.$$

It would seem that the main reason for the discrepancy in tim ing and rate of oxygen consumption is an overestimate in the clad ding temperatures at the hottest location as oxidation begins. We note that if the above H_2/O_2 reaction were very rapid then hydro gen and oxygen would not be observed together. The minor over lap between oxygen and hydrogen points to oxidation by steam occurring at some locations across the bundle before oxygen was fully consumed at others, and to finite rate mixing of the gases.

The observed hydrogen production rate is less (ca. 20%) than the observed total steam consumption. If measurement uncertainty is not an issue then absorption and dissolution in the metallic Zirca loy (not modelled) seems the most likely explanation.

Somewhat fortuitously, the cases in which the reduction factor is applied gave excellent agreement with data for the total hydro gen production with both choices of steam oxidation correlation (CP/UH and Ls/PC). This was not strongly influenced by the faster PC kinetics compared with UH since the steam was fully consumed for most of this time. As regards the oxidation state of the bundle at initiation of reflood these cases are preferred to the standard PSI model for air oxidation, even if the modelling of oxidation in a steam/air(oxygen) mixture is questionable.

Finally, the absence of a model for nitriding somewhat under mines the interpretation of the behaviour during the time of nitro gen uptake. The nitrogen also impacts the bundle conditions for reflood in ways that cannot be analysed by the code models. The observed onset of nitrogen uptake occurred only after all the oxy gen was consumed but slightly before all the steam was consumed. Theoretical considerations strongly suggest that the nitride does not form unless the oxygen partial pressure is effectively zero at the metal oxide interface, so that steam would also inhibit the nitriding, as observed experimentally (Steinbrück and van Appeldorn, 2018). Like the situation at the onset of oxygen starva tion, the simultaneous uptake of nitrogen and steam in the offgas line appears to be due to local starvation.

5.3. Reflood phase

The reflood phenomenology is analysed via the post hoc chosen base case (3) together with the variants (1, 2, 4, 5, 6, 7, 8) intro duced in Section 4.

Cases 1 and 2 are rather aside from the reflood modelling since oxygen is not present. They mostly affect the reflood signatures via the greater previous oxidation compared with the data and with the other simulations. Comparison between cases 1 and 2 shows a lasting impact on the oxide layer due to the nitrogen.

Case 4 is counterpart to 3 except that the Ls/PC correlation is used instead of CP/UH. These cases differ pre reflood mostly because of the slower steam oxidation kinetics (case 4) at temper atures below about 1300 K; during reflood they differ because of the faster kinetics at temperatures above about 1800 K. Although PC gives closer agreement for the total oxidation during reflood, neither case captures the initial temperature increase or the hydro gen generation, so the relative level of agreement between these cases cannot be used to justify for a preference for PC over UH. Case 4 comes closest to reproducing the data over the whole experiment without radically altering the boundary conditions. This case is regarded as the best estimate and is the one included in the QUENCH 18 post test benchmark exercise (Hollands, 2018).

Case 5 assumes no oxide layer breach until the cladding tem perature reaches 2500 K and hence effectively suppresses the breakout of metallic melt and its exposure to the flowing steam. The much reduced hydrogen generation points strongly to oxida tion of exposed metallic melt as a driver for the excursion. How ever, other processes which are not modelled perhaps also promoted oxidation during the experiment, such as dissolution of oxide during oxidant starvation or mechanical damage to the rods due to contact with reflood water.

Case 6 supposes no effect of the shroud breach on the net injec tion and argon flow in the bundle. The intact shroud case is clearly unrealistic, as evidenced by the much more rapid refill and quench progression. It is included as a sensitivity to demonstrate the impact of the breach on refill/quench progression and the excur sion. As regards the other cases, a more faithful representation of the breach would be to include a pathway through the shroud to and from the region containing insulating material behind the shroud. However, the uncertain nature of the breach and the extre mely complex thermal hydraulic and material interaction makes this impractical. It is not possible to model the shroud breach pro cess itself using the present code version.

None of the above simulations come close to the scale of oxida tion during reflood. In fact despite the large differences in mod elling, the span of results is much smaller than the underestimation of oxidation. A serious limitation is the lack of any treatment for nitriding and its reoxidation. The total hydrogen contribution is about 40 g based on the release of nitrogen. Although a significant amount it does not directly account for the calculation data discrepancy for any of the cases, although the reoxidation was a source of heat and may also have synergised with the metallic oxidation. More crucially, the calculations indi cate that the oxidation was essentially steam limited while most of the hydrogen was generated, and this is also suggested by the observed reflood signatures. There would seem to have been a large steam flow through the bundle during the early period of reflood, and therefore some mechanism for generating the steam.

Cases 7 and 8 include additional steam flow postulated on the basis of observed signatures. Such a large steam flow would have

been simultaneously a driver for the oxidation and a coolant. The contrast between these calculated results suggests that additional steam during high temperature reflood would not necessarily enhance the excursion it would depend on other factors which can be lumped together as the ignitability of bundle. One such factor is the oxidation kinetics. Case 7 (CP/UH correlation) is counterpart of the base case (3) and shows no additional oxidation instead extra cooling during time of steam flow. Case 8 (Ls/PC correlation) is coun terpart to case 4 and shows a temperature increase and a large hydrogen release, in remarkably close to the data. These simulations were performed to help the interpretation of the observed beha viour. Case 8 cannot properly be regarded as best estimate, since there is no independent evidence to support the magnitude of addi tional steam flow. The possibility of debris water interaction that was alluded to in Section 3 is a credible scenario which could, in prin ciple, be simulated with sufficiently complete modelling.

The comparison with experiment suggests that there was rapid steam generation and that the bundle was (due to whatever cause) sufficiently ignitable for the oxidation heat to dominate over the cooling. The comparison suggests that the PC kinetics might be an improvement over UH. Although it works well in these analyses, it is possible that other limitations of the modelling meant that some of the drivers for excursion were not captured. It might be that the fast PC kinetics simply tipped the scales back onto the side of a bigger excursion. Therefore any conclusion about the relative merits of PC and UH should be regarded as provisional, pending more complete modelling of the other processes.

6. Conclusions

A series of simulations of QUENCH 18 was performed to address modelling issues and to interpret the observed experimen tal sequence.

The sequence is particularly complicated, comprising sequential steam preoxidation, oxidation in a steam air mixture with starva tion of both oxidant species, nitriding, a reflood excursion with major oxidation of Zircaloy, reoxidation of nitride, and significant damage to the test section. The sequence necessarily poses a strin gent test of modelling capability.

The best estimate case gives generally good agreement for the pre reflood phases, as well as significant reflood oxidation, although modelling of the reflood remains problematic.

Comparisons between the various sensitivity cases shed helpful light on some of the key processes and modelling issues during all phases of the experiment.

The analyses indicate a number of modelling issues further development and study:

(1) The most notable limitation is the absence of any treatment for the formation and reoxidation of zirconium nitride. The lack of a model compromises the simulation of sequences that include nitriding.
(2) There is no specific modelling of oxidation in a steam air mixture. The current assumption that steam is an inert spe cies in the presence of oxygen is probably incorrect.
(3) The analyses tend to support the idea of a reduced oxidation rate at low oxygen concentration, but this may be incorrect in a steam air mixture.
(4) There is indication that some of the hydrogen produced by nitrogen affected oxidation in steam may be taken up into the underlying Zircaloy. Hydrogen dissolution and hydriding may have consequences in some situations.
(5) Breakout of metallic melt from the breached oxide layer and its oxidation is an important driver for an excursion and needs to be modelled. Oxide breach can currently be treated parametrically in SCDAPSim.
(6) The analyses tend to support the adoption of the Leistikow and Prater Courtright correlations as credible alternatives, to Cathcart Pawel and Urbanic Heidrick (default in SCDAP sim). However, since the modelling of high temperature oxi dation, starvation, and nitrogen effects are currently incomplete, it may be wise to analyse accident sequences with each correlation.

This assessment of modelling capability should be regarded as provisional, pending fuller characterisation of the experimental sequence and the state of the test section, followed continued anal yses with the current models. However, the lack of a nitriding model, the sensitivity of reflood simulation to the oxidation kinet ics and to the criterion for onset of relocation degradation have implications for use in reactor analyses. Considerable care is there fore required in addressing modelling uncertainties and in the interpretation of results. The issues identified above for SCDAPSim also apply at least to some extent to all the BDBA analysis codes.

Acknowledgments

The QUENCH 18 experiment was supported by the KIT program NUSAFE and partly sponsored by the ALISA project. The bundle materials were provided by AREVA.

References

Adorni, Martina, Herranz, Luis E., Hollands, Thorsten, Ahn, Kwang-Il, Bals, Christine, D'Auria, Francesco, Horvath, Gabor L., Jaeckel, Bernd S., Kim, Han-Chul, Lee, Jung-Jae, Ogino, Masao, Techy, Zsolt, Velazquez-Lozad, Alexander, Zigh, Abdelghani, Rehacek, Radomir, 2016. OECD/NEA Sandia Fuel Project phase I: Benchmark of the ignition testing. Nucl. Eng. Des. 307, 418–430. https://doi.org/10.1016/j.nucengdes.2016.07.016.

Birchley, J., Clèment, B., Löffler, H., Tromm, W., Amri, A., 2010. Outcome of the OECD/SARNET Workshop on In-vessel Coolability. In: Proceedings of 4th European Review Meeting on Severe Accident Research (ERMSAR-2010), Bologna (Italy), May 11–12, 2010. http://www.sar-net.eu/sites/default/files/ERMSAR_2010/Papers/Paper-S3-1.pdf.

Birchley, Jonathan, Fernandez-Moguel, Leticia, 2012. Simulation of air oxidation during a reactor accident sequence: Part 1 – Phenomenology and model development. Ann. Nucl. Energy 40 (1), 163–170. https://doi.org/10.1016/j.anucene.2011.10.019.

Duriez, C., Dupont, T., Schmet, B., Enoch, F., 2008. Zircaloy-4 and M5® high temperature oxidation and nitriding in air. J. Nucl. Mater. 380 (1-3), 30–45. https://doi.org/10.1016/j.jnucmat.2008.07.002.

Fernandez-Moguel, Leticia, Birchley, Jonathan, 2012. Simulation of air oxidation during a reactor accident sequence: Part 2 – Analysis of PARAMETER-SF4 air ingress experiment using RELAP5/SCDAPSIM. Ann. Nucl. Energy 40 (1), 141–152. https://doi.org/10.1016/j.anucene.2011.10.018.

Fernandez-Moguel, Leticia, Birchley, Jonathan, 2013. Analysis of QUENCH-10 and -16 air ingress experiments with SCDAPSim3.5. Ann. Nucl. Energy 53, 202–212. https://doi.org/10.1016/j.anucene.2012.08.030.

Große, Mirco, Lehmann, Eberhard, Steinbrück, Martin, Kühne, Guido, Stuckert, Juri, 2009. Influence of oxide layer morphology on hydrogen concentration in tin and niobium containing zirconium alloys after high temperature steam oxidation. J. Nucl. Mater. 385 (2), 339–345. https://doi.org/10.1016/j.jnucmat.2008.12.021.

Grosse, M., 2010. Comparison of the high-temperature steam oxidation kinetics of advanced cladding materials. Nucl. Technol. 170 (1), 272–279. https://doi.org/10.13182/NT10-A9464.

Grosse, Mirco, Steinbrueck, Martin, Schillinger, Burkhard, Kaestner, Anders, 2018a. In situ Investigations of the Hydrogen Uptake of Zirconium Alloys during Steam Oxidation. ASTM Special Technical Publication, pp. 1114–1135. STP 1597 https://doi.org/10.1520/STP159720160041.

Grosse, M., Pulvermacher, S., Steinbrück, M., Schillinger, B., 2018b. In-situ neutron radiography investigations of the reaction of Zircaloy-4 in steam, nitrogen/steam and air/steam atmospheres. Physica B: Condens. Matter 551, 244–248. https://doi.org/10.1016/j.physb:2018.03.030.

Hering, W., Homann, Ch., Lamy, J.-S., Miassoedov, A., Schanz, G., Sepold, L., Steinbrück, M., 2002. Comparison and interpretation report of the OECD international standard problem no.45 exercise (QUENCH-06). Forschungszentrum Karlsruhe Report FZKA 6722. https://publikationen.bibliothek.kit.edu/270052469/3814240.

Hering, W., Homann, Ch., 2007. Improvement of the SCDAP/RELAP5 Code with Respect to FZK Experimental Facilities. Forschungszentrum Karlsruhe, Report FZKA 6566. https://publikationen.bibliothek.kit.edu/270068455/3814999.

Hofmann, P., Homann, C., Leiling, W., Miassoedov, A., Piel, D., Schanz, G., Schmidt, L., Sepold, L., Steinbrück, M., 2000. Experimental and Calculational Results of the Experiments QUENCH-02 and QUENCH-03. Forschungszentrum Karlsruhe, Report FZKA 6295, July 2000. https://publikationen.bibliothek.kit.edu/270048148/3813990.

Hollands, Thorsten, 2017. Pre-Test Benchmarks in the Frame of the NUGENIA QUESA Project: QUENCH-ALISA and CODEX-AIT3. In: Proceedings of 23rd International QUENCH Workshop, Karlsruhe, October 2017. https://doi.org/10.5445/IR/1000076201.

Hollands, Thorsten, 2018. First Results of the QUENCH-18 Post-Test Benchmark in the Frame of the NUGENIA QUESA Project. In: Proceedings of 24th International QUENCH Workshop, Karlsruhe 2018. https://doi.org/10.5445/IR/1000088229.

Hózer, Z., Windberg, P., Nagy, I., Maróti, L., Matus, L., Horváth, M., Pintér, A., 2002. CODEX-AIT-1 Experiment: Core Degradation Test under Air Ingress. AEKI Budapest, KFKI-2002-02/G. http://real.mtak.hu/12865/1/1236158.pdf.

Leistikow, S., Schanz, G., Berg, H.V., Aly, A.E., 1983. Comprehensive presentation of extended Zircaloy-4 steam oxidation results (600–1600 °C). In: OECD/NEA-CSNI/IAEA Meeting, Risø, Denmark, May 1983, IAEA Summary Report IWGFPT/16. http://www.iaea.org/inis/collection/NCLCollectionStore/_Public/15/059/15059438.pdf?r=1.

Madokoro, Hiroshi, Erkan, Nejdet, Okamoto, Koji, 2015. Assessment of the models in RELAP/SCDAPSIM with QUENCH-06 analysis. J. Nucl. Sci. Technol. 52 (11), 1417–1424. https://doi.org/10.1080/00223131.2015.1005717.

Pawel, R.E., Cathcart, J.V., McKee, R.A., et al., 1979. The kinetics of oxidation of zircaloy-4 in steam at high temperatures. J. Electrochem. Soc. 126, 1105–1111. https://doi.org/10.1149/1.2129227.

Schanz, G., Adroguer, B., Volchek, A., 2004. Advanced treatment of zircaloy cladding high-temperature oxidation in severe accident code calculations. Nucl. Eng. Des. 232 (1), 75–84. https://doi.org/10.1016/j.nucengdes.2004.02.013.

Sepold, L., Hering, W., Homann, C., Miassoedov, A., Schanz, G., Stegmaier, U., Steinbrück, M., Steiner, H., Stuckert, J., 2004a. Experimental and Computational Results of the QUENCH-06 Test (OECD ISP-45) Forschungszentrum Karlsruhe, Report FZKA 6664, February 2004. https://publikationen.bibliothek.kit.edu/270057214/3814496.

Siefken, L.J., Coryell, E.W., Harvego, E.A., Hohorst, J.K., Arndt, S.A., 1997. SCDAP/RELAP5/MOD3.2 Code Manual. USNRC NUREG/CR-6150 Rev. 1, INEL-96/0422, Idaho. National Engineering Laboratories. https://www.nrc.gov/docs/ML0103/ML010370328.pdf.

Steinbrück, M., Homann, C., Miassoedov, A., Schanz, G., Sepold, L., Stegmaier, U., Steiner, H., Stuckert, J., 2004a. Results of the B4C Control Rod Test QUENCH-07. Forschungszentrum Karlsruhe, Report FZKA 6746, May 2004. https://publikationen.bibliothek.kit.edu/270058023/3814536.

Steinbrück, M., Miassoedov, A., Schanz, G., Sepold, L., Stegmaier, U., Steiner, H., Stuckert, J., 2004b. Results of the QUENCH-09 Experiment with a B4C Control Rod. Forschungszentrum Karlsruhe, Report FZKA 6829, December 2004. https://publikationen.bibliothek.kit.edu/270059406/3814615.

Steinbrück, Martin, Miassoedov, Alexei, Schanz, Gerhard, Sepold, Leo, Stegmaier, Ulrike, Stuckert, Juri, 2006. Experiments on air ingress during severe accidents in LWRS. Nucl. Eng. Des. 236 (14–16), 1709–1719. https://doi.org/10.1016/j.nucengdes.2006.04.010.

Steinbrück, Martin, 2009. Prototypical experiments relating to air oxidation of Zircaloy-4 at high temperatures. J. Nucl. Mater. 392 (3), 531–544. https://doi.org/10.1016/j.jnucmat.2009.04.018.

Steinbrück, M., Große, M., Sepold, L., Stuckert, J., et al., 2010. Synopsis and outcome of the QUENCH experimental program. Nucl. Eng. Des. 240, 1714–1727. https://doi.org/10.1016/j.nucengdes.2010.03.021.

Steinbrück, M., Gerhards, U., Grosse, M., Leiste, H., Prestel, S., Stegmaier, U., et al., 2011. Recent results of KIT separate-effects tests on oxidation of zirconium alloy claddings. In: Proceedings of 17th Int. QUENCH Workshop, Karlsruhe, Nov. 2011, ISBN 978-3-923704-77-4.

Steinbrück, Martin, Schaffer, Steffi, 2016. High-temperature oxidation of zircaloy-4 in oxygen-nitrogen mixtures. Oxidation Metals 85 (2016), 245–262. https://doi.org/10.1007/s11085-015-9572-1.

Steinbrueck, Martin, da Silva, Fabio Oliveira, Grosse, Mirco, 2017. Oxidation of zircaloy-4 in steam-nitrogen mixtures at 600–1200 °C. J. Nucl. Mater. 490, 226–237. https://doi.org/10.1016/j.jnucmat.2017.04.034.

Steinbrück, Martin, van Appeldorn, Philipp, 2018. Comparative high-temperature oxidation tests with zircaloy-4 in various atmospheres. In: Proceedings of the Topfuel Conference 2018.

Stuckert, J., Steinbrück, M., 2014. Experimental results of the QUENCH-16 bundle test on air ingress. Progr. Nucl. Energy 71, 134–141. https://doi.org/10.1016/j.pnucene.2013.12.001.

Stuckert, J., Hózer, Z., Kiselev, A., Steinbrück, M., 2016. Cladding oxidation during air ingress. Part I: Experiments on air ingress. Ann. Nucl. Energy 93, 4–17. https://doi.org/10.1016/j.anucene.2015.12.034.

Stuckert, J., Steinbrück, M., Kalilainen, J., Lind, T., Zhang, Y., 2018. First results of the QUENCH-ALISA bundle test. In: Proceedings of NUTHOS-12, paper 918, Qingdao/China, October 2018. https://doi.org/10.5445/IR/1000087684.

Uetsuka, H., Hofmann, P., 1985. Reaction Kinetics of Zircaloy-4 in a 25% O_2/75% Ar Gas Mixture from 900 to 1500°C under Isothermal Conditions. Forschungszentrum Karlsruhe, Report KfK 3917, May 1985. https://publikationen.bibliothek.kit.edu/270021279/3812896.

Urbanic, V.F., Heidrick, T.R., 1978. High temperature oxidation of zirclaoy-2 and zircaloy-4 in steam. J. Nucl. Mater. 75, 251–261. https://doi.org/10.1016/0022-3115(78)90006-5.

Vryashkova, P., Groudev, P., Stefanova, A., 2013. Sensitivity study of Quench-16 experiment with MELCOR computer code. In: Proceedings of 19th Int. QUENCH Workshop, Karlsruhe, Nov. 2013, ISBN 978-3-923704-84-2.